

[advances.sciencemag.org/cgi/content/full/6/50/eabc4704/DC1](https://advances.sciencemag.org/cgi/content/full/6/50/eabc4704/DC1)

## Supplementary Materials for

### **A biomimetically hierarchical polyetherketoneketone scaffold for osteoporotic bone repair**

Bo Yuan, Linnan Wang, Rui Zhao, Xi Yang, Xiao Yang\*, Xiangdong Zhu\*, Limin Liu, Kai Zhang, Yueming Song, Xingdong Zhang

\*Corresponding author. Email: [xiaoyang114@scu.edu.cn](mailto:xiaoyang114@scu.edu.cn) (X.Y.); [zhu\\_xd1973@scu.edu.cn](mailto:zhu_xd1973@scu.edu.cn) (X.Z.)

Published 11 December 2020, *Sci. Adv.* **6**, eabc4704 (2020)  
DOI: 10.1126/sciadv.abc4704

#### **This PDF file includes:**

Supplementary Materials and Methods  
Figs. S1 to S8  
Tables S1 and S2

## **Supplementary Materials**

### **Materials and Methods**

#### **Compressive mechanical properties**

Uniaxial compression tests were performed on the cylindrical samples ( $4 \times 7 \text{ mm}^3$ ) to evaluate mechanical properties of PEKK scaffolds using a materials testing machine (Instron 8875, Norwood, MA, USA). A compressive load was applied to each sample at a crosshead speed of 0.5 mm/min until the sample was destroyed. The compressive strength and elastic modulus were calculated and reported based on the force-displacement data. Five parallel samples of each group were used in the tests.

#### **Apatite formation**

In order to investigate the ability to form bone-like apatite, the PEKK samples were immersed in stimulated body fluid (SBF) at 37 °C for 1, 4 and 7 days. The SBF contains 142.0 mM Na<sup>+</sup>, 5.0 mM K<sup>+</sup>, 2.5 mM Ca<sup>2+</sup>, 1.5 mM Mg<sup>2+</sup>, 148.8 mM Cl<sup>-</sup>, 4.2 mM HCO<sub>3</sub><sup>-</sup>, and 1.0 mM HPO<sub>4</sub><sup>2-</sup> and is buffered at pH 7.40 by 50 mM Tris-buffer and 45 mM HCl.

#### **Isolation and culture of osteoporotic osteoblasts**

All procedures in the experiment were approved by the Institutional Animal Care and Use Committee of Sichuan University. Five female Sprague Dawley rats aged 8 weeks ( $200 \pm 20 \text{ g}$ ) were purchased from Laboratory Animal Center of Sichuan University (Chengdu, China). Cell experiments were carried out using the osteoblastic cells derived from osteoporotic rat bone by the following methods. In brief, all the rats were acclimatized for 14 days under standard condition (25 °C, 12 hours light/dark cycles) and given a bilateral ovariectomy. After 3 months, rats were sacrificed by an overdose of pentobarbital sodium and tibia bones were harvested. The excised tibia was cut into small explants with length of 1-2 mm after removing soft tissues and bone marrow. Before being placed in 6-well tissue culture plates, the bone explants were washed in penicillin/streptomycin (Gibco, USA) solution for 5 times to remove bone marrow attached. DMEM supplemented with 10% standard foetal bovine serum (FBS, Gibco, USA), 1% penicillin/streptomycin and 100 μM L-Ascorbate (Sigma Aldrich, USA) was used throughout this study. The 6-well tissue culture plates were maintained at 37 °C in a humidified incubator under 5% CO<sub>2</sub>. During the culture time, osteoporotic osteoblasts gradually migrated from the surface of bone explants and attached to the culture plate.

#### **Cell morphology and viability**

On day 1, 4 and 7, the cells were stained with fluorescein diacetate (FDA, Sigma, USA) for live cells (green) and propidium iodide (PI, Sigma, USA) for dead cells (red) after being washed twice with PBS. The morphology of cell on different groups of materials was observed using SEM. Prior to observing, the samples were fixed in 2.5% glutaraldehyde for 12 h and rinsed with PBS two times, and then dehydrated in ascending concentrations of alcohols from 30% to 100%. For further observing morphology and quantifying cell area, cells were stained with Phalloidin-TRITC (Sigma) and 4',6-Diamidino-2-phenylindole dihydrochloride (DAPI, Sigma) to visualize cytoskeleton and the cell nucleus. The mean area of single cell was quantitatively evaluated by using Image Pro Plus 6.0 software (Media Cybernetic, USA), in which six randomized non-overlapping fields in each sample were selected.

At each time point, the cells were washed with PBS two times and incubated with 200  $\mu\text{L}$  of MTT (5 mg/mL in PBS) for 4h at 37  $^{\circ}\text{C}$ . After incubation, the solution was removed and dimethyl sulfoxide (DMSO) was added to dissolve the purple formazan salts. Finally, the solution was centrifuged to remove the nanoparticles before being transferred into a 96-well plate. The optical density (O. D.) was measured at a wavelength of 490 nm by a multifunctional, full-wavelength microplate reader (Varioskan Flash, Thermo Scientific, USA). For the above assays, all experiments were performed in triplicate.

### Surgical procedure

The animal experiments were approved by the Institutional Animal Care and Use Committee of Sichuan University. The rats were anaesthetized by intraperitoneal injection of pentobarbital (Nembutal 2 mg/100 g). A sagittal incision was made on the skins of the distal femoral and then the femoral condyle was exposed by blunt dissection. A cylindrical hole (diameter: 3 mm and depth: 4 mm) was created perpendicular to the distal femur of rats by using a dental drill with low rotational drill speed. Finally, the femoral condyle defects were generated and randomly filled with sample. All the rats as-operated were evenly distributed into three groups including PEKK, nHA/PEKK and nSrHA/PEKK. After surgery, two fluorochromes, i.e. tetracycline (30 mg/kg at 14 and 13 days before death, Sigma) and calcein (6 mg/kg at 4 and 3 days before death, Sigma) were administered to assess the osseogenic activity at 4, 8 and 12 weeks. At each time point, the rats were euthanized by an intraperitoneal overdose injection of pentobarbital. The harvested bone specimens were fixed in a 4% paraformaldehyde solution for 7 days before further analysis.

### Supplementary Figures

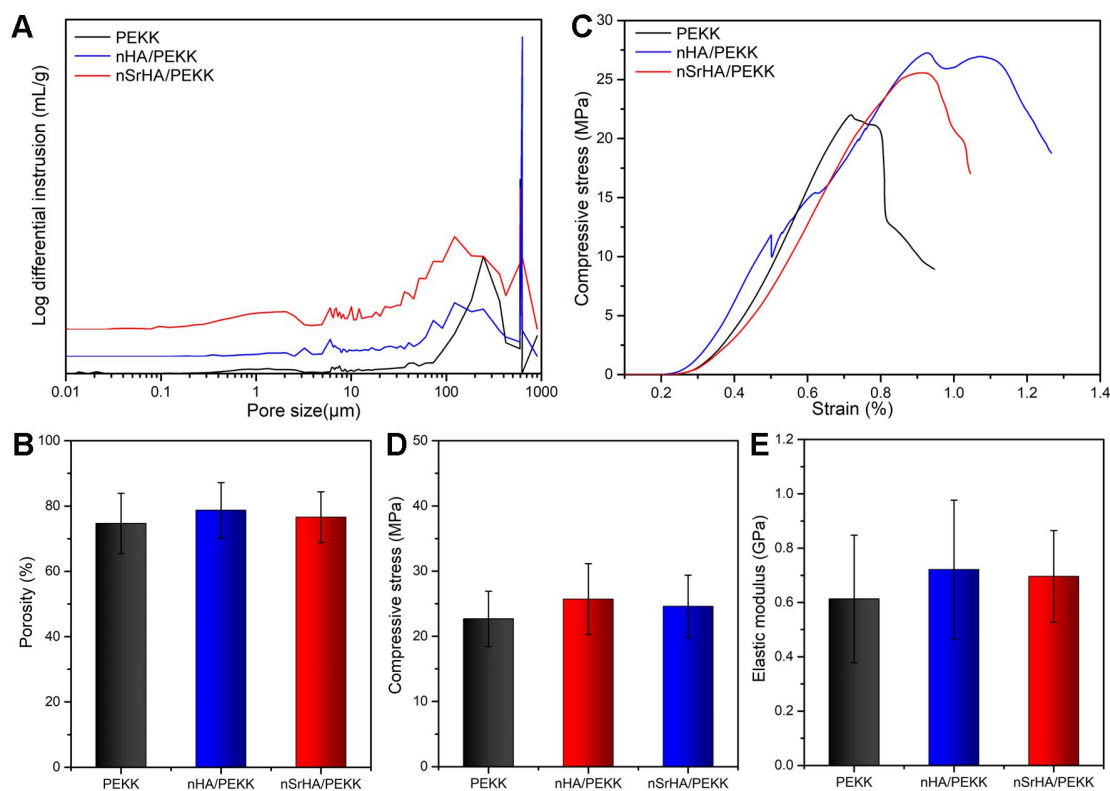


**Fig. S1. Macroporous structure and compressive mechanical properties of PEKK scaffolds.** (A) Porosities and (B) pore size distribution of PEKK scaffolds. (c) Representative compressive stress-strain curves, (D) compressive strength and (E) elastic modulus of

PEKK scaffolds. (error bars, mean  $\pm$  SD. n=3 per group for mercury intrusion porosimetry and n=5 per group for compressive mechanical tests, \*  $p < 0.05$  significant as compared to PEEK, #  $p < 0.05$  significant as compared to nHA/PEEK). All analyses done using one-way ANOVA with Tukey's post hoc test.

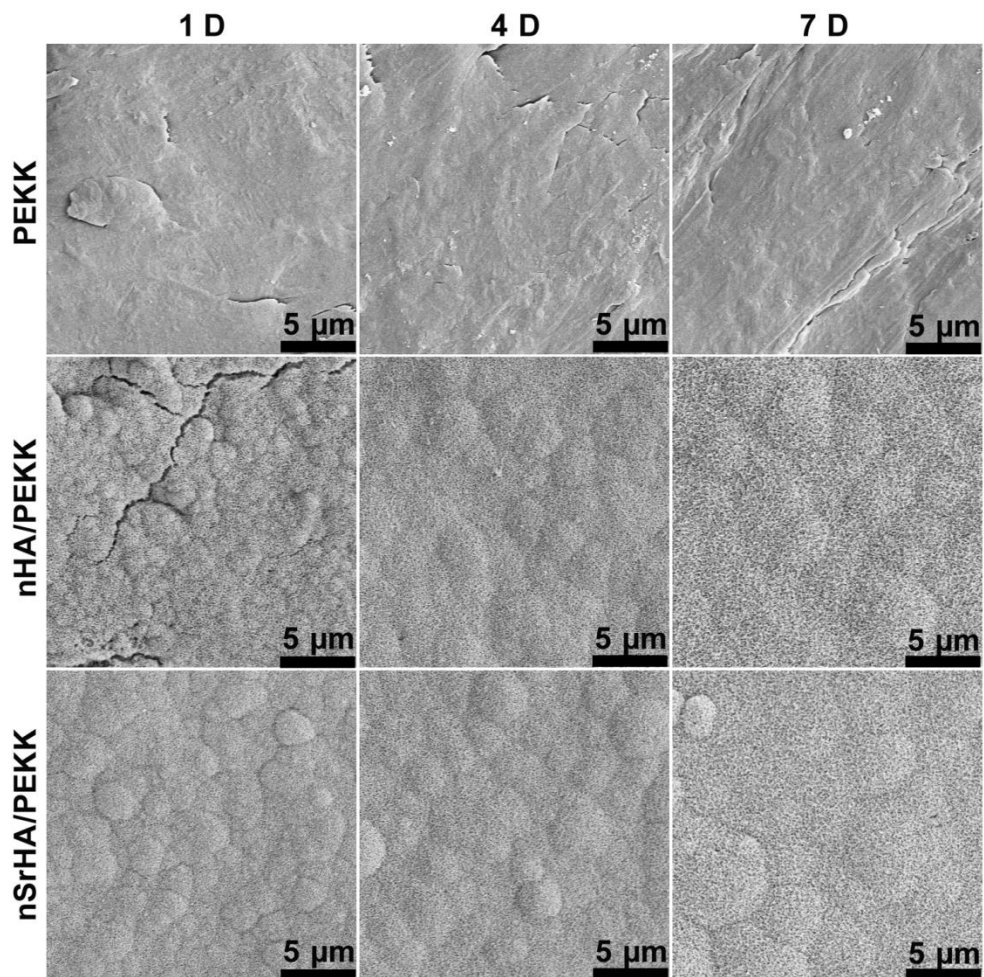
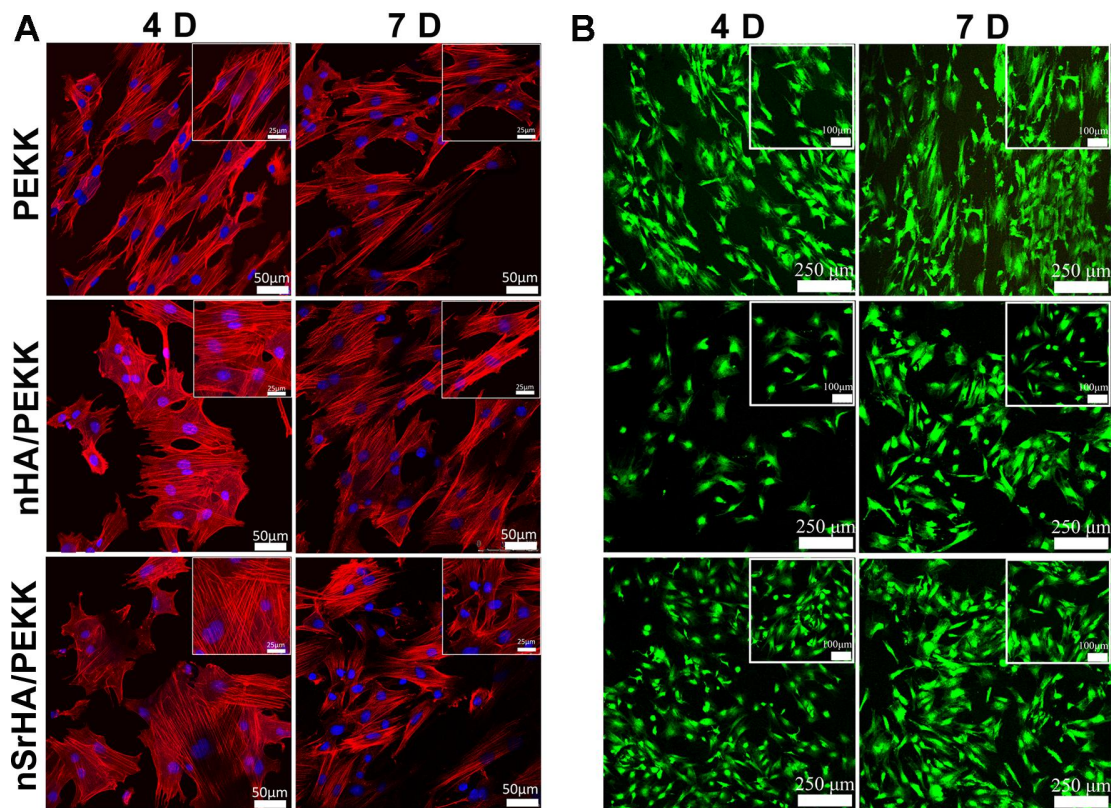
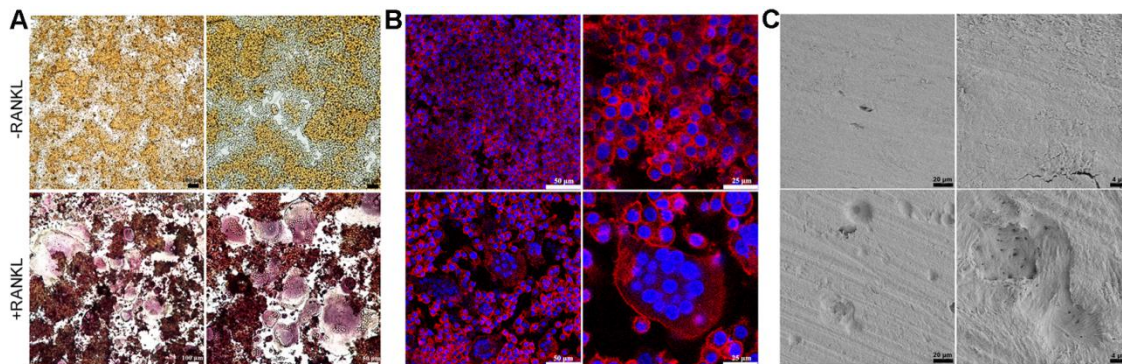


Fig. S2. SEM images of PEKK scaffolds after soaking SBF for 1, 4 and 7 days.



**Fig. S3. Cell morphology observation of osteoporotic osteoblasts cultured on various PEKK scaffolds for 4 and 7 days. (A)** Fluorescence images of osteoporotic osteoblasts with F-actin stained with Phalloidin-TRITC (red) and nuclei stained with DAPI (blue). **(B)** Fluorescence images of live (green) /dead (red) staining of osteoporotic osteoblasts.



**Fig. S4. Osteoclasts formation from Raw264.7 cells after 4 days treatment with RANKL.** All cultures were supplemented with 100 ng/ml RANKL. **(A)** Trap staining for Raw264.7 cells. Trap-positive cells with at least three nuclei were considered osteoclasts. **(B)** Representative fluorescence images showing large multinucleated osteoclasts with typical ring-like F-actin sealing zones. **(C)** Representative SEM images of resorption pits on bovine bone slices produced by bone resorbing multinucleated osteoclasts.

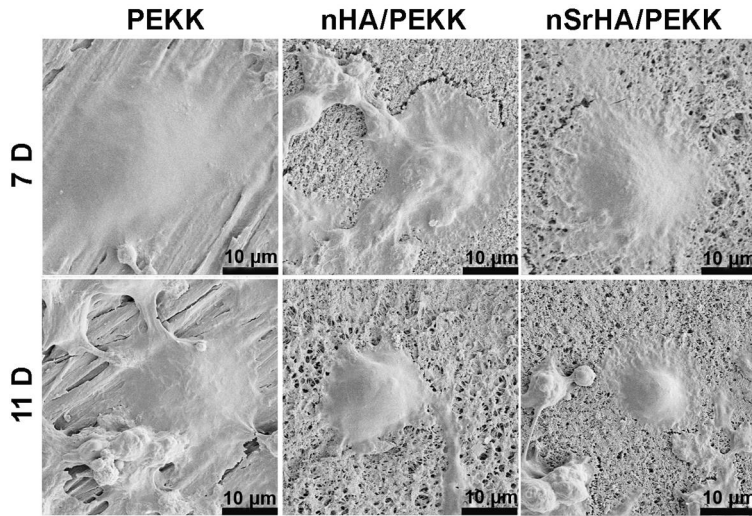


**Fig. S5.** SEM images of RAW264.7 cells mediated by RANKL cultivated for 7 and 11 days on various PEKK scaffolds.

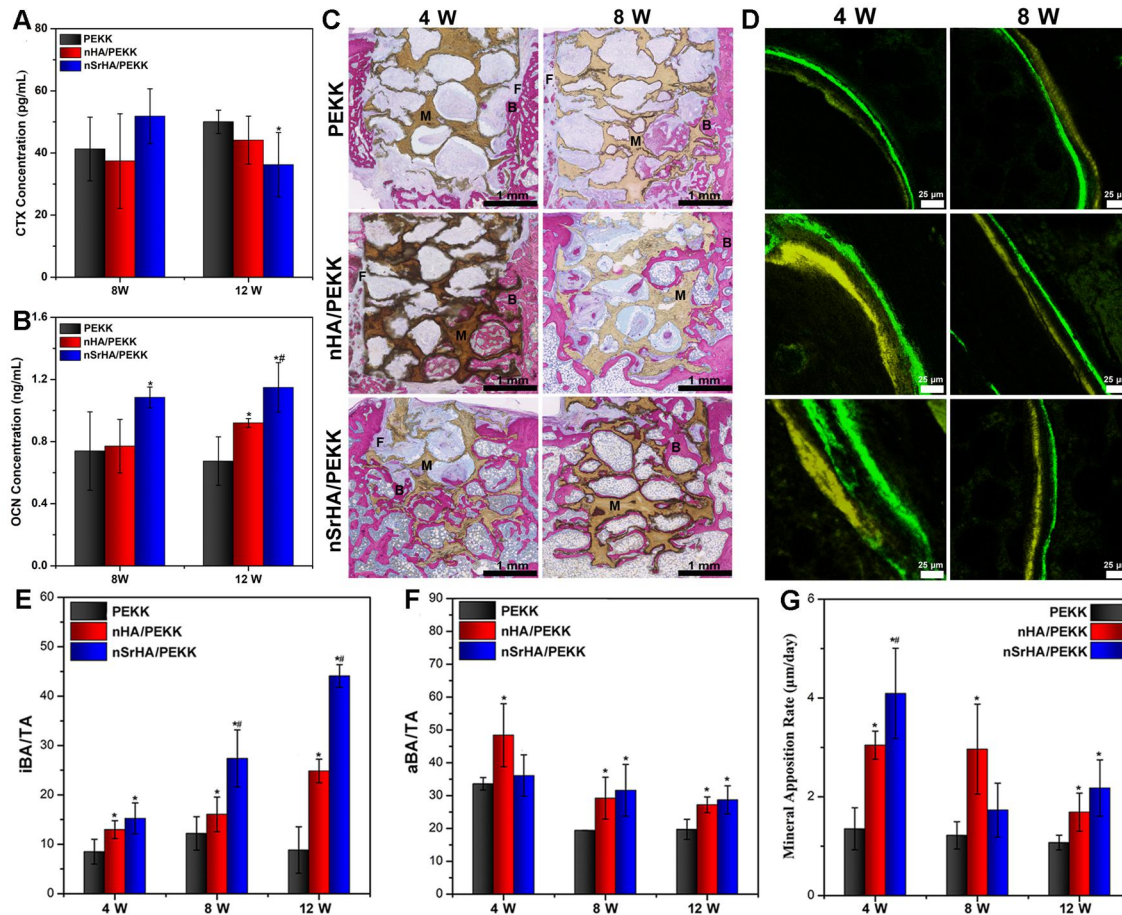


**Fig. S6. Biochemical detection and histological observation for osteoporotic bone regeneration.** (A) The serum level of CTX and (B) OCN change acquired from the OVX-rats including various PEKK scaffolds at 8 and 12 weeks postoperatively. (C) The typical light microscopic images of H&E stained histological sections of the PEKK samples at 4 and 8 weeks postoperatively (M: Material; B: Bone tissue; F: Fibrous tissue). (D) Sequential fluorescent labeling observation at 4 and 8 weeks postoperatively (M: material, Yellow: labeling by tetracycline, Green: labeling by tetracycline calcein). Quantitative analysis of (E) new bone area to tissue area ratio within the porous scaffolds, (F) adjacent

to the implant, (G) mineral apposition rate after 4, 8 and 12 weeks of implantation. (error bars, mean  $\pm$  SD.  $n=5$  per group, \*  $p < 0.05$  significant as compared to PEEK, #  $p < 0.05$  significant as compared to nHA/PEEK). All analyse done using one-way ANOVA with Tukey's post hoc test.

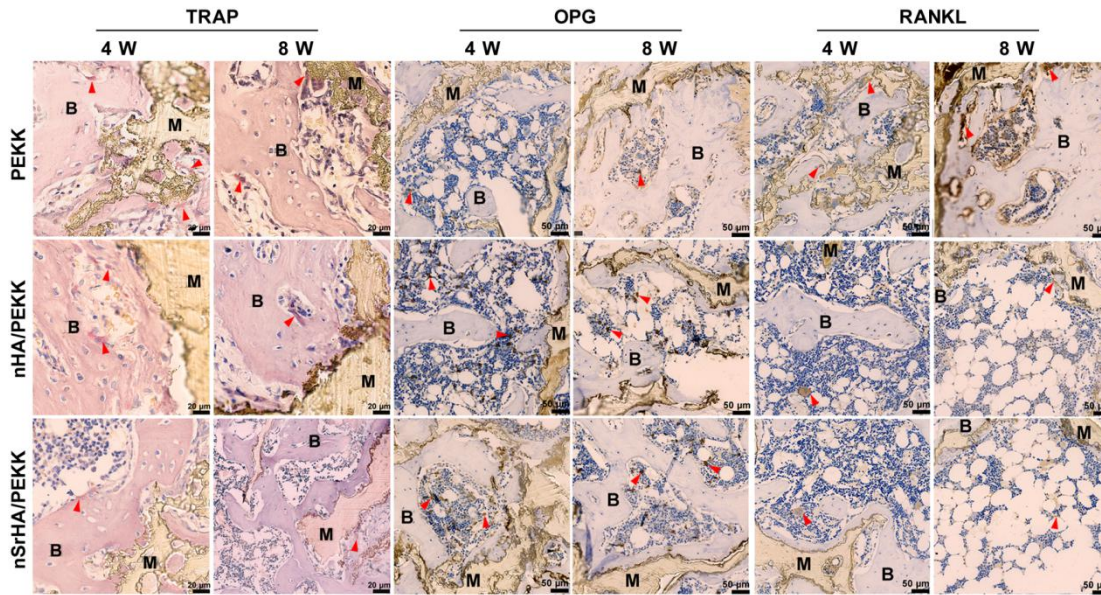


**Fig. S7.** TRAP, RANKL and OPG staining of histological sections from different groups at week 4 and 8 postoperatively (M: Material, B: Bone Tissue, Arrow: Osteoclast).

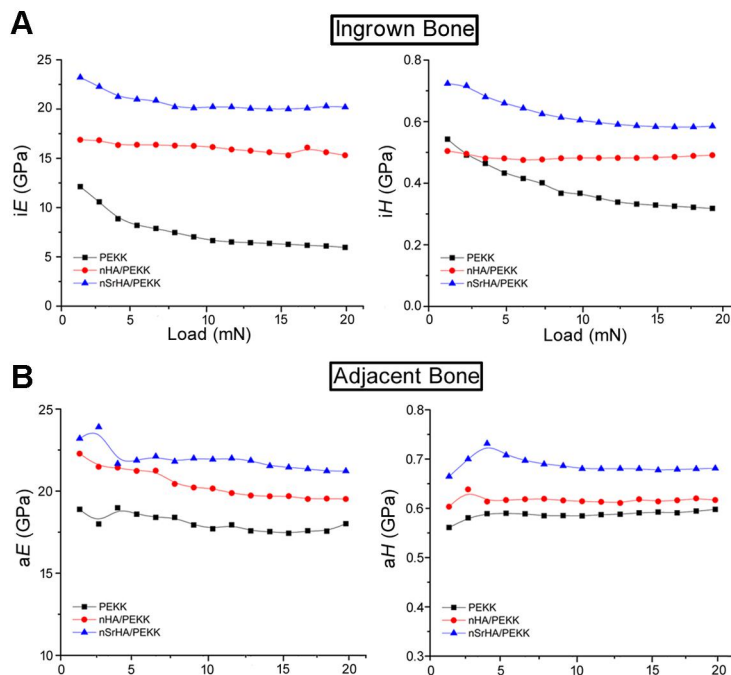


**Fig. S8.** Effect of different scaffolds on new bone strength at micro-level. (A) Typical load-elastic modulus ( $iE$ ) curves and load-hardness ( $iH$ ) curves generated from cyclic nanoindentation testing on ingrown new bone. (B) Typical load-elastic modulus ( $aE$ ) curves and load-hardness ( $aH$ ) curves generated from cyclic nanoindentation testing on adjacent new bone (dotted red line: stiffness).

**Table S1. Surface element compositions of the PEKK scaffolds.**

Samples	C, at.%	O, at.%	S, at.%	P, at.%	Ca, at.%	Sr, at.%
PEKK	81.40±1.75	19.20±1.37	—	—	—	—
nHA/PEKK	49.99±3.85	36.85±4.02	0.94±0.01	4.60±0.23	7.62±0.04	—
nSrHA/PEKK	53.86±0.26	34.69±0.45	0.91±0.07	3.95±0.33	5.95±0.4	0.64±0.05

**Table S2. Osteogenesis and osteoclastogenesis related gene primer pairs used in the qRT-PCR.**

Target	forward primer	Reverse primer
ALP	ATGGTAACGGGCTGGCTACA	AGTTCTGCTCATGGACGCCGT
BSP	CCAGCCAGGACTGCCGAAGG	CGCTGCCTCCCTGGACTGGA
Runx2	AGATGGGACTGTGGTTACCG	GGACCGTCCACTGTCACCTT
VEGF	AGAAGGGGAGCAGAAAGCCC	AGTGACGTTGCTCTCCGACG
OCN	CCTGGCAGGTGCAAAGCCCA	GGGGGCTGGGGCTCCAAGT
OPG	TGTCCCTTGCCCTGACTACT	TTCCTCACATTCGCACACTC
RANKL	GGGAGCACTAAGAACTGGTCA	AACAGGGAAGGGTTGGACAC
GAPDH-1	ACCCAGAAGACTGTGGATGG	CAGTGAGCTTCCCCTTCAG
NFATc1	CCGTTGCTTCCAGAAAATAACA	TGTGGGATGTGAACTCGGAA
Cath-K	CTTCCAATACGTGCAGCAGA	TCTTCAGGGCTTTCTCGTT
c-fos	CCAGTCAAGAGCATCAGCAA	AAGTAGTGCAGCCCGGAGTA
MMP-9	CAAAGACCTGAAAACCTCCAA	GGTACAAGTATGCCTCTGCCA
TRAP	CTGGAGTGCACGATGCCAGCGACA	TCCGTGCTCGGCGATGGACCAGA
CAII	ACTGGGGATACAGCAAGCAC	AAAGGAGTGGCCGTTGTTGA
GAPDH-2	TGGTGAAGGTCGGTGTGAAC	CCATGTAGTTGAGGTCAATGAAGG